



HAL
open science

Dataset for H₂, CH₄ and organic compounds formation during experimental serpentinization

Fang Huang, Samuel Barbier, Renbiao Tao, Jihua Hao, Pablo Garcia del Real, Steve Peuble, Andrew Merdith, Vladimir Leichnig, Jean-philippe Perrillat, Kathy Fontaine, et al.

► To cite this version:

Fang Huang, Samuel Barbier, Renbiao Tao, Jihua Hao, Pablo Garcia del Real, et al.. Dataset for H₂, CH₄ and organic compounds formation during experimental serpentinization. *Geoscience Data Journal*, 2020, 8 (1), pp.90-100. 10.1002/gdj3.105 . hal-04818632

HAL Id: hal-04818632

<https://hal.science/hal-04818632v1>

Submitted on 5 Dec 2024

HAL is a multi-disciplinary open access archive for the deposit and dissemination of scientific research documents, whether they are published or not. The documents may come from teaching and research institutions in France or abroad, or from public or private research centers.

L'archive ouverte pluridisciplinaire **HAL**, est destinée au dépôt et à la diffusion de documents scientifiques de niveau recherche, publiés ou non, émanant des établissements d'enseignement et de recherche français ou étrangers, des laboratoires publics ou privés.



Distributed under a Creative Commons Attribution 4.0 International License



Dataset for H₂, CH₄ and organic compounds formation during experimental serpentinization

Fang Huang^{1,2} | Samuel Barbier^{3,4} | Renbiao Tao³ | Jihua Hao³ |
Pablo Garcia del Real³ | Steve Peuble³ | Andrew Merdith³ | Vladimir Leichnig³ |
Jean-Philippe Perrillat³ | Kathy Fontaine¹ | Peter Fox¹ | Muriel Andreani³ |
Isabelle Daniel³

¹Tetherless World Constellation, Rensselaer Polytechnic Institute, Troy, NY, USA

²CSIRO Mineral Resources, Kensington, WA, Australia

³Univ Lyon, Univ Lyon 1, ENSL, CNRS, LGL-TPE, Villeurbanne, France

⁴Total CSTJF, Pau, France

Correspondence

Fang Huang, CSIRO Mineral Resources, Kensington, 26 Dick Perry Ave, WA 6151, Australia.

Email: f.huang@csiro.au

Funding information

TOTAL EP R&D Project MAFOOT; Deep Carbon Observatory through Alfred P. Sloan Foundation, Grant/Award Number: G-2018-11204

Abstract

Serpentinization refers to the alteration of ultramafic rocks that produces serpentines and secondary (hydr)oxides under hydrothermal conditions. Serpentinization can generate H₂, which in turn can potentially reduce CO/CO₂ and produce organic molecules via Fischer–Tropsch type (FTT) and Sabatier type reactions. Over the last two decades, serpentinization has been extensively studied in laboratories, mainly due to its potential applications in prebiotic chemistry, origin of life in extreme environments, development of carbon-free energies and CO₂ sequestration. However, the production of H₂ and organics during experimental serpentinization is hugely variable from one publication to another. The experiments span over a large range of pressure and temperature conditions, and starting compositions of fluid and solid phases are also highly variable, which collectively adds up to more than a hundred variables and leads to controversial results. Therefore, it is extremely difficult to compare results between studies, explain their variability and identify key parameters controlling the reactions. To overcome these limitations, we collected and analysed 30 peer-reviewed articles including over 100 experimental parameters and ca. 30 mineral and organic products, hence building up a database can be completed and

Huang and Barbier are co-first authors

Dataset

Identifier: <http://info.deepcarbon.net/individual/n1819>

Creators: Samuel Barbier, Fang Huang, Renbiao Tao, Jihua Hao, Pablo Garcia del Real, Steve Peuble, Andrew Merdith, Vladimir Leichnig, Valentine Megevand, Jean-Philippe Perrillat, Isabelle Daniel, Muriel Andreani

Title: Dataset for H₂, CH₄ and Organic Compounds Formation during Experimental Serpentinization

Publisher: Deep Carbon Observatory

Publication year: 2019

Resource type: Dataset

Version: 1.0

This is an open access article under the terms of the Creative Commons Attribution License, which permits use, distribution and reproduction in any medium, provided the original work is properly cited.

© 2020 The Authors. *Geoscience Data Journal* published by Royal Meteorological Society and John Wiley & Sons Ltd.

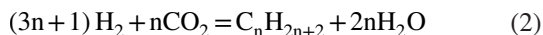
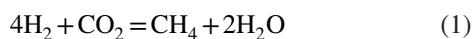
implemented in future studies. We then extracted basic statistical information from this dataset and demonstrate how such a comprehensive dataset is essential to better interpret available data and discuss the key parameters controlling the effectiveness of H₂, CH₄ and other organics production during experimental serpentinization. This is essential to guide the design of future experiments.

KEYWORDS

abiotic hydrogen, abiotic methane, experimental serpentinization, hydrothermal

1 | INTRODUCTION

Earth's mantle is predominantly composed of peridotites, a type of rock made of Mg- and Fe-rich silicate minerals such as olivine and pyroxene. Though modern Earth's crust is not ultramafic, plate tectonics bring ultramafic rocks to the surface of Earth at various geologic settings, such as slow mid-ocean ridges (e.g. Mid Atlantic Ridge, Southwest Indian Ridge), oceanic transform faults (e.g. Vema OTF in the Atlantic, São Pedro and São Paulo Archipel OTFs in the Equatorial Atlantic, Shaka and Prince Edward OTFs in the South-West Indian Ocean) and at convergent margins (e.g. Oman, New Caledonia). The alteration and hydration of peridotite result in the formation of serpentine group minerals (e.g. lizardite, chrysotile and antigorite) and secondary (hydr)oxides (e.g. brucite, magnetite). These serpentine-forming reactions are called serpentinization. During serpentinization, the ferrous iron in olivine and pyroxene is often oxidized to ferric iron, which produces H₂ through the reduction of water. As a consequence, CO or CO₂ could be reduced by H₂ through Sabatier type (R1) or Fischer–Tropsch type (R2) reaction to form CH₄ and/or other organic compounds.



Analyses of many natural samples have shown abundant release of H₂, CH₄ and other organic compounds in fluids from natural serpentinization areas and questioned the exact reactions mechanisms involved (Barnes *et al.*, 1967; Wenner and Taylor, 1973; Charlou *et al.*, 2002; Proskurowski *et al.*, 2006, 2008; Konn *et al.*, 2009). For instance, ultramafic rocks were abundant on the primitive Earth and possibly other rocky planetary bodies (Ehlmann *et al.*, 2010; Zahnle *et al.*, 2011; Holm *et al.*, 2015; Etiopie *et al.*, 2018), so their observation raises several major scientific questions related to serpentinization (Sleep *et al.*, 2004; Schulte *et al.*, 2006; Russell *et al.*, 2010; Hellevang *et al.*, 2011; Guillot and Hattori, 2013; Mayhew *et al.*, 2013; McCollom and Seewald, 2013; Brazil,

2017; Ménez *et al.*, 2018): What is the role of serpentinization in the origin of life—on Earth, and elsewhere? Could the serpentinization reaction sustain microbial communities in the primitive and modern ocean? Could our modern societies use the H₂ produced by serpentinization reactions to help reduce anthropogenic CO₂ emission?

To address these questions, there is an urgent need to understand the serpentinization process and more specifically its capacity to generate reducing conditions and produce abiotic organics. Therefore, tens of experiments have attempted to provide answers to this question. Although they all agree on the production of H₂ by serpentinization (Sleep *et al.*, 2004; Seyfried *et al.*, 2007), the production of CH₄ and more complex hydrocarbons (e.g. C₂H₆, C₃H₈) via FTT or Sabatier reactions has always been and is still highly debated (e.g. Evans *et al.*, 2013; McCollom and Seewald, 2013; McCollom *et al.*, 2015). Despite the tremendous collaborative efforts of the community all over the world, we still do not fully understand why similar experimental incentives lead to so contrasted, if not contradictory results. A strong limitation is that those numerous serpentinization experiments have been run under very different conditions using various creative protocols. In order to understand the similarities and discrepancies between results, it requires us to compare more than a hundred variables not even fully identified before the present study. Therefore, we carefully read 30 peer-reviewed publications that described experimental serpentinization and other publications for comparison, analysed 195 experiments and compiled parameters in the dataset described in Section 2. This dataset will be continuously updated as news results become available and used for various purposes related to serpentinization and associated reactions.

2 | DATASET DESCRIPTION

2.1 | Overview of the dataset

We have collected the data in 30 relevant experimental articles that report measured H₂ and organic compounds (OC) production related to the serpentinization reaction (Berndt *et al.*,

Article's informations		Experimental conditions										
Title of the Publication	Authors et al XXXX	Number of individual experiments	Temperature /Pressure	Duration at each analyses	Rock type (not precise if less than 5% different)	Mineralogy composition wt%	Initial knows catalyst(s)	Degree of alteration	Grainsize	Surface area	Solution composition	Initial pH
Title	Author et al., XXXX	N°	Kelvin/MPa	Hours	name or description, and origin	Olivine (Mg#(OI)), Pyroxene (Cpx, Opx), Spinel, Magnetite, Chromite, Serpentine, Brucite, SiO ₂ , Chlorite, Phlogopite, Talc, oxides, sulfurs, ... wt%	Spinel, Magnetite, Alloys, ... yes or no	Fresh, Medium altered, or Highly altered	min and MAX μm	XXXX cm ² /gram of rock	NaCl, CO ₂ , CH ₄ , CO (dissolved), NaHCO ₃ , HCOOH, KCl, CaCl ₂ , MgCl ₂ ,... mol-mmol/kg	X

Experimental conditions										Results			
Mass solids and liquid	W/R ratio	Gas composition	Origin of the carbon source	Reactor type	Reactor composition	State of initial phases adds	Blank in the experimental set up	Intermediate sampling	Final pH	Reaction extent (0=>1)	Minerals formation's composition	Gases and liquids formations	
X g	X	N ₂ , CO ₂ , H ₂ , Ar,... %	In the solid, liquid and or gases phase(s)	Flexible, Parr type, Glass bottle,...	Gold, Titanium, alloys, Teflon, Borosilicates, ...	Solids, and/or Liquids, and/or Gases	yes or no	yes or no	X	X	Phyllosilicate, Chrysotile, Lizardite, Antigorite, Talc, Brucite, Magnetite, Chromite, Carbonate, Siderite, Hematite, Pentlandite, Heazlewoodite, Reduced carbon...	H ₂ , CH ₄ , CO ₂ , O ₂ , C ₂ H ₆ , C ₃ H ₈ , NOX, NH ₄ , C ₂ H ₄ , C ₃ H ₆ , Formate, Acetate, Propionate, Other organics mol-mmol/kg	

FIGURE 1 Screenshot of a representative version of the Excel spreadsheet for experimental parameters and results. The current dataset has 134 columns (parameters/variables) and 733 rows (measurements). The dataset is divided into three parts—article information, experimental conditions and results

1996; Horita and Berndt, 1999; McCollom and Seewald, 2001; McCollom and Seewald, 2003; Allen and Seyfried, 2003; Foustoukos and Seyfried, 2004; Seewald *et al.*, 2006; Seyfried *et al.*, 2007; Fu *et al.*, 2007, 2008; Ji *et al.*, 2008; Dufaud *et al.*, 2009; Jones *et al.*, 2010; McCollom *et al.*, 2010, 2016; Marcaillou *et al.*, 2011; Neubeck *et al.*, 2011, 2014; Lafay *et al.*, 2012; Lazar *et al.*, 2012, 2015; Klein and McCollom, 2013; Okland *et al.*, 2014; Klein *et al.*, 2015; Huang *et al.*, 2015, 2016; McCollom, 2016; McCollom and Donaldson, 2016; Miller *et al.*, 2017; Grozeva *et al.*, 2017). The vast majority of these studies report on experimental serpentinization starting with olivine or peridotites, but a couple of studies are included in the dataset on purpose, to investigate FTT reactions without olivine as a starting mineral (Foustoukos and Seyfried, 2004; Fu *et al.*, 2007; Ji *et al.*, 2008). The latter bypasses the serpentinization reaction and uses formic acid, which decomposes into H₂ and CO/CO₂ at temperatures and pressures similar to those typical of hydrothermal serpentinization and could react to form abiotic organic compounds.

The reported experiments covered a large range of experimental conditions, including the temperature (T), pressure (P), experiment duration, chemical compositions of both reactants and products, as well as types of reactors, origins

of mineral samples. We summarized the information into a single large Excel spreadsheet of 133 columns and 733 rows. The spreadsheet columns are divided into 3 main sections (Figure 1): article information (green header), experimental conditions (blue header); and results (yellow header). The section on article information includes details of all published articles of this dataset: data ID, article title, year of publication, authors and DOI numbers, which help the readers of the present contribution to trace back the original studies. The 733 rows describe 195 experiments that include sometimes multiple samplings on the course of the experiments to evaluate the reaction kinetics.

Before moving into the details of each section of the dataset, there is some important general information. In the section dedicated to experimental conditions, it is important to keep in mind that most parameters are independent of each other, but a few of them are dependent. For example, the magnesium content of olivine 'Mg#(OI)' displays a value only for experiments that include olivine as a reactant. Another example, the total of the reacting minerals sums at 100% and is expressed as wt%. In order to analyse the dataset, a feature is assigned to each cell as explained in the header of each column.

Parameters	Min	Max	Average	Number of 'nan'	Data type
No_of_experiments	1	22	–	0	Numeric
Temperature_C	25	500	217.55	0	Numeric
Pressure_MPa	0	350	40.04	0	Numeric
Duration_hr	0	20,499	1647.58	0	Numeric

Parameters	Number of 0	Number of 1	Average	Number of 'nan'	Data type
Reactor_Flexible_autoclave	321	412	–	0	Binary
Reactor_Parr_type	728	5	–	0	Binary
Bottle_in_oven	549	184	–	0	Binary
Reactor_Au	281	452	–	0	Binary
Reactor_Au/Ti	371	362	–	0	Binary
Reactor_Ti	370	363	–	0	Binary
Reactor_Hastelloy	728	5	–	0	Binary
Reactor_Glass	495	238	–	0	Binary
Reactor_Platinum	718	15	–	0	Binary
Reactor_Teflon_Plastic	473	260	–	0	Binary

Some programs cannot handle dataset with empty cells, so we assigned 'nan' (not a number) to values that were either not measured or not reported, and '0' to measurements that were below detection limits or reported as 'not observed' in the original paper. We also paid attention to assign to each parameter a dedicated format that is given in Tables 1-9 of the present contribution:

1. Numeric: data that are integers and float numbers. For example, temperature data are mostly integers and NaCl concentration data are float numbers.
2. Categorical: data that are not quantitative but categories, such as the rock type and degree of alteration.
3. Binary: Data that are either 0 (no) or 1 (yes), such as the reactor types.
4. Ternary: Data that are 0 (no), 1 (yes) or 2 (yes with ^{13}C). For example, in the Carbon_in_solid column, 2 means carbon is ^{13}C labelled.

2.2 | Experimental parameters

2.2.1 | Reaction conditions and reactor information

The reaction conditions are listed first in Table 1: temperature (T) ranges between 25 and 500°C, pressure (P) between 0.1 and 350 MPa, and experimental durations are between 0 and 20,499 hrs. In most experiments, intermediate sampling was

performed to study reaction kinetics and thus is reported in the dataset as a parameter—0 means no intermediate sampling performed whilst 1 means that the experiments were sampled through time. With 733 measurements and 195 experiments, each experiment on average takes 3.75 measurements.

Different types of reactors are used depending on the experimental P-T conditions, experimental protocols and sample volumes (Table 2). The reactor materials are also indicated since they are made of metals, whose catalytic role has often been suggested. For each experiment, one of the columns dedicated to the nature of the reactor has a value of 1, others are 0. For instance, a reactor made of both Au and Ti corresponds to '1' in the column Reactor_Au/Ti, other columns display a '0' for that experiment.

2.2.2 | Starting mineral, fluid and gas compositions

The information on the composition of rocks, minerals, solutes in the aqueous phase and gas is summarized in Tables 3-5. Table 3 contains the provenance of samples, the type of rock, the degree of alteration (when indicated by the authors), the composition of the rocks (expressed in weight per cent of each mineral normalized to reach 100%), the Mg# (olivine only), the grain size and other information on the starting mineral phases that we considered useful. The provenance of a sample is either its original geological location or the name of the company where it was synthesized. The estimated degree of alteration is based on

TABLE 1 Summary of experimental conditions, pressure, temperature, duration and number of experiments. Temperature is in °Celsius, pressure in MPa and duration in hours

TABLE 2 Statistics and information on the type of reactors used for experimental serpentinization

TABLE 3 Summary of starting mineral compositions and relevant parameters

Parameters	Min	Max	Average	Number of 'nan'	Data type
Provenance_of_sample	–	–	–	0	Categorical
Rock_type	–	–	–	0	Categorical
Degree_of_alteration	–	–	–	73	Categorical
Olivine_wt%	0	100.00	49.50	33	Numeric
Mg#(Ol)	0	92	70.28	231	Numeric
Clinopyroxene_wt%	0	40	1.52	5	Numeric
Orthopyroxene_wt%	0	100	4.13	5	Numeric
Pyroxene_wt%	0	100	5.38	0	Numeric
Spinel_wt%	0	5	0.25	0	Numeric
Magnetite_wt%	0	100	4.30	0	Numeric
Haematite_wt%	0	92.6	0.76	0	Numeric
Serpentine_wt%	0	100	3.37	0	Numeric
Brucite_wt%	0	6	0.30	0	Numeric
Talc_wt%	0	1	0.05	0	Numeric
Carbonate_wt%	0	0.25	0.01	0	Numeric
Amphibole_wt%	0	5	0.09	0	Numeric
Chlorite_wt%	0	1	0.02	0	Numeric
Phlogopite_wt%	0	1	0.05	0	Numeric
Chromite_wt%	0	100	2.00	0	Numeric
Clinocllore_wt%	0	1	0.04	0	Numeric
GLASS	0	75	1.39	0	Numeric
SiO ₂ _wt%	0	100	0.82	0	Numeric
Fe_wt%	0	100	5.59	0	Numeric
NiFe_wt%	0	100	6.92	0	Numeric
FeO_wt%	0	100	1.34	0	Numeric
Fes_wt%	0	50	0.35	0	Numeric
NiO_wt%	0	50	0.34	0	Numeric
Grain_size_min	0	300	51.88	195	Numeric
Grain_size_max	0	3,000	213.04	207	Numeric
SSA	0	71,000	7832.77	535	Numeric

mineral descriptions in the original articles—fresh (nearly 0% altered), altered (nearly 100% altered) and medium altered. The missing values for the degree of alteration are mainly from experiments started without a mineral phase, which are dedicated to carbon speciation at high P and T. Information of grain size (max and min) and surface area (SSA, cm²/g of rock) that are very important for the kinetics of the reaction is also reported in this section when available, otherwise they are labelled as 'nan'. Simple statistics analyses of these parameters are displayed in Tables 3-5, which helps readers to decide if this dataset contains useful data for them.

The chemical composition of the starting aqueous solution is described in Table 4. The solutes include many organic and inorganic salts whose concentrations are given in mol/kg (molal) as volumes change significantly under hydrothermal

conditions. When articles reported in their experimental section that milli-Q water (18.2 MΩ/cm) was used, the column 'precised_water_clean' displays a value of '1', otherwise the value is '0'. Values of the pH of the starting solution are also given as 'initial pH' when available. The initial amount of carbon among starting chemicals is one important aspect in this study, which allows comparing between studies the produced reduced carbon compounds through FTT or Sabatier reactions or any other reaction. We created a column 'CO₂_initial' that tells whether authors flushed their system or not. If not, we assumed that fluids were at equilibrium with present day atmospheric CO₂, which leads to a CO₂ concentration of 0.01 millimole per kg H₂O.

When an experiment contained a headspace filled with gas, we reported as much as we could the gas composition. It is given in relative volume percentage of N₂, CO₂, H₂, CO, CH₄

TABLE 4 Starting fluid chemical compositions and relevant parameters

Parameters	Number of 0	Number of 1	Average	Number of 'nan'	Data type
Precised_water_clean	270	463	–	0	Binary
Parameters	Min	Max	Average	Number of 'nan'	Data type
NaCl_molal	0	1.71	0.287	0	Numeric
CH ₄ _initial_mmolal	0	24	0.098	0	Numeric
CO_initial_mmolal	0	80	1.746	0	Numeric
CO ₂ _initial_mmolal	0	200	6.968	0	Numeric
HCO ₃ _mmolal	0	2.2	0.158	0	Numeric
NaHCO ₃ _molal	0	0.172	0.008	0	Numeric
HCOOH_molal	0	0.37	0.026	0	Numeric
KCl_molal	0	0.034	0.004	0	Numeric
CaCl ₂ _molal	0	0.1	0.004	0	Numeric
MgCl ₂ _molal	0	0.6	0.021	0	Numeric
NH ₄ Cl_molal	0	0.019	0.001	0	Numeric
K ₂ HPO ₄ _molal	0	2.87E-04	1.55E-05	0	Numeric
KNO ₃ _molal	0	5.01E-05	2.46E-06	0	Numeric
Ca(OH) ₂ _molal	0	1.00E-04	4.92E-06	0	Numeric
CaSO ₄ ·H ₂ O_molal	0	2.00E-04	9.82E-06	0	Numeric
Mg(SO ₄) ₂ ·7H ₂ O_molal	0	5.00E-05	2.48E-06	0	Numeric
C ₂ H ₂ O ₄ _molal	0	2.25E-04	2.64E-06	0	Numeric
NaOH_molal	0	1.00	0.03	0	Numeric
Initial_pH	2	13.50	6.50	319	Numeric

TABLE 5 Starting gas compositions

Parameters	Min	Max	Average	Number of 'nan'	Data type
Gas_N ₂ %	0	100	29.90	0	Numeric
Gas_CO ₂ %	0	100	4.07	0	Numeric
Gas_H ₂ %	0	100	0.14	0	Numeric
Gas_CO%	0	100	2.18	0	Numeric
Gas_CH ₄ %	0	100	0.41	0	Numeric
Gas_Ar%	0	100	0.68	0	Numeric

and Ar in the headspace, as the description in the experiment methods section in the articles seldom provided detailed information on the gas composition (Table 5). For each experiment, the initial concentrations of these gases are therefore reported as vol%, and the sum of these species in the headspace equals arbitrarily 100% or 0 when information is missing.

2.2.3 | Potential catalysts and carbon sources

Previous studies (Fu *et al.*, 2008; Andreani *et al.*, 2013; Mayhew *et al.*, 2013) have shown that the serpentinization reaction and

the production of H₂ and organic species (CH₄, formate, acetate, etc.) can be largely influenced by the presence of cations in solution or solid catalysts (accessory mineral surfaces). In industrial H₂ and CH₄ production, metal-bearing catalysts are critical. Platinum, rhodium, ruthenium, cobalt and other metallic materials are well-known catalysts for methanization of dry gas by FTT or Sabatier reaction (McKee, 1967; Melaet *et al.*, 2014; Stangeland *et al.*, 2017). In natural environments, a large number of metallic phases are present in ultramafic rocks and minerals, and also in experimental materials as impurities. Variabilities of the kinetics of serpentinization and H₂ and CH₄ formation, both in nature and experiments, could be due to the effect of catalysts either in their mineral form or as solute (e.g. Andreani *et al.*, 2013; Mayhew *et al.*, 2013; Etiope and Ionescu, 2015). Therefore, we created a list of minerals with potential or expected catalytic effects and recorded their presence or absence in each experiment (Table 6).

The carbon source(s) are also recorded in the dataset in a 'ternary' data format (definition in section 2) for two main goals here: (a) identify if the amount of reduced carbon products is favoured by certain carbon-bearing reactants; (b) help readers to easily locate experiments labelled with ¹³C and further analyse the influence of background contaminations.

TABLE 6 Potential catalysts and carbon source

Parameters	Number of 0	Number of 1	Number of 2	Average	Number of 'nan'	Data type
Catalyst_Spinel	571	162	–	–	0	Binary
Catalyst_Magnetite	603	130	–	–	0	Binary
Catalyst_Chromite	584	149	–	–	0	Binary
Catalyst_Ni_bearing	628	105	–	–	0	Binary
Catalyst_Fe_bearing	624	109	–	–	0	Binary
Carbon_in_Solid	688	45	0	–	0	Ternary
Carbon_in_Liquid	172	429	132	–	0	Ternary
Carbon_in_Gas	584	121	28	–	0	Ternary

TABLE 7 Other information related to experimental conditions

Parameters	Number of 0	Number of 1	Average	Number of 'nan'	Data type
isBlank	609	124	–	0	Binary
Add_Solids	140	593	–	0	Binary
Add_Liquids	0	733	–	0	Binary
Add_Gases	478	255	–	0	Binary
Intermediate_sampling	167	566	–	0	Binary

Parameters	Min	Max	Average	Number of 'nan'	Data type
Total_volume_ml	0.31	250.00	81.82	412	Numeric
Mass_solids	0	120	10.70	42	Numeric
Mass_liquids	0	180	37.58	92	Numeric
Water_Rock	0	400	13.26	170	Numeric

TABLE 8 Mineral products of experimental results

Parameters	Number of 0	Number of 1	Average	Number of 'nan'	Data type
Chrysotile_product	330	74	–	328	Binary
Lizardite_product	444	28	–	261	Binary
Antigorite_product	471	0	–	262	Binary
Phyllosilicate_product	325	134	–	274	Binary
Talc_product	293	10	–	430	Binary
Brucite_product	354	44	–	335	Binary
Magnetite_product	219	96	–	418	Binary
Haematite_product	180	0	–	553	Binary
Chromite_product	249	15	–	469	Binary
Pentlandite_product	263	2	–	468	Binary
Heazlewoodite_product	225	4	–	504	Binary
Carbonate_product	145	67	–	521	Binary
Siderite_product	129	7	–	597	Binary
Iowaite_product	261	10	–	462	Binary
Ni_Fe_phase_product	170	62	–	501	Binary
Reduced_carbon_product	52	17	–	664	Binary
Unidentified_phase_product	132	17	–	584	Binary

TABLE 9 H₂ and other organic products in final fluids

Parameters	Min	Max	Average	Number of 'nan'	Data type
H ₂ _mM	0	2170.25	66.534	82	Numeric
CH ₄ _mM	0	58.2	0.859	189	Numeric
C ₂ H ₆ _mM	0	0.71	0.058	513	Numeric
C ₂ H ₄ _mM	0	0.3	0.026	600	Numeric
C ₃ H ₆ _mM	0	0.45	0.034	602	Numeric
C ₃ H ₈ _mM	0	0.33	0.040	535	Numeric
C ₄ _mM	0	0.3	0.055	647	Numeric
C ₅ _mM	0	0.2	0.032	647	Numeric
C ₆ _mM	0	0.13	0.017	648	Numeric
Formate_mM	0	257	27.344	590	Numeric
CH ₃ OH_mM	0	9	1.179	664	Numeric
Acetate_mM	0	114	3.980	669	Numeric
Propionate_mM	0.0002	0.0136	0.006	722	Numeric
CO ₂ _mM	0	2287.88	35.95	317	Numeric
Alk_meq_mM	0	10.40	1.13	699	Numeric
Final_pH	0	13.50	7.57	339	Numeric

2.2.4 | Other information

All other information regarding the starting materials is listed in Table 7. The 'isBlank' parameter indicates whether an experiment is blank or control (1 for no mineral within a series of experiments), in order to distinguish them from experiments and avoid any inaccurate interpretation of the data. The 'Add_solids', 'Add_liquids' and 'Add_gases' are used to indicate the presence of a solid, liquid or gas phase, respectively (0 means absent). The 'mass_solids', 'mass_liquids' and 'Water_rock' ratio are also reported when available, as well as the total volume of the reaction cells.

3 | RESULTS

The results section of the dataset is divided into two subsections—mineral and gas/fluid products. The columns that describe mineral products are less populated, since most contributions focused on the production of gas species (H₂, CH₄, etc.) and only a few of them also described the kinetics of serpentinization and analysed the final mineral composition.

3.1 | Mineral products

Analyses of mineral products are reported in Table 8. It includes all the minerals identified by the authors of the 30

peer-reviewed articles. Each mineral produced during experiments is defined as a parameter, and reading through the columns, one can see that the data available in the literature are sparse. As a consequence, statistics on the minerals produced during the reaction is poorly constrained. The presence or absence of secondary minerals is not always clearly established in the articles and strongly depends on the details provided by the authors and characterization technique used in those contributions. In some cases, descriptions of the solid phase did not mention the experiment number they were referring to. In addition, in most experimental settings dedicated to the understanding of H₂ and CH₄ production during serpentinization, solids are accessible only at the end of the experiments. The mineral feature is assigned 'nan' if the information is not clearly stated. Hence, this part of the dataset should be used with great care and we encourage the reader to refer to the original article as necessary.

3.2 | H₂ and hydrocarbon products in final fluids

This subsection focuses on the experimental measurements of H₂, CH₄ and OC during experimental serpentinization. We assigned an individual parameter to each compound. The details on the analysis of the composition of final fluids are described in Table 9. It is important to take into account that the measurement precision and detection limit of those compounds are very different across studies and potentially evolved through time as analytical tools and methods improve. Obviously, the

most commonly measured species are H₂ and CH₄, given the topic. Other organic species are measured only in a few studies and have therefore many missing values (nan) in the dataset. Though each organic compound is listed in its own column, all species other than H₂ and CH₄ shall be combined in order to perform some meaningful data analysis.

4 | DISCUSSIONS AND PERSPECTIVES

This dataset provides an up-to-date collection of experimental results until early 2019 that can be used to address the implications of serpentinization and related processes for the production of H₂, CH₄ and higher hydrocarbons. It is well known that P-T conditions largely control experimental results, but they alone could not explain the large variability of the measured concentrations of H₂, CH₄ and higher hydrocarbons. The other parameters investigated by the experimental community at large are so numerous that their investigation cannot be done easily and requires a computing approach that can deal with many parameters at the same time. We hope that the database is progressively enriched with upcoming experimental results. As an example, we have used data science techniques to extract embedded information and identify key experimental parameters, which cannot be accessed by checking a limited number of parameters.

In our recent paper (Barbier *et al.*, 2020), we used network analysis and machine-learning algorithms to analyse a processed version of this dataset. We found that, as previously known, pressure and temperature are the two most important parameters that govern the production of H₂ and OC. However, we did not find evidences to support the occurrence of R1 or R2 reactions. Moreover, by comparing the concentrations of final OC with initial carbon input, we found that the OC products in several studies are from unidentified sources and likely result from contamination, in agreement with the scarce ¹³C-labelled studies (e.g. McCollom *et al.*, 2010; Grozeva *et al.*, 2017). Also, the measurements of initial and final pH values are often not reported, despite the important role of pH on the serpentinization kinetics (e.g. Huang *et al.*, 2019; McCollom *et al.*, 2020). More information and the detailed analytical methods can be found in Barbier *et al.* (2020). The dataset can also be extended to other reactions under similar conditions using different solid reactants, such as mine-tailing products, to produce H₂, CH₄ and other carbon species (e.g. Kularatne *et al.*, 2018; Michiels *et al.*, 2018; Brunet, 2019). We hope that this dataset and the analysis by Barbier *et al.* (2020) stimulate complementary experiments that could fill the identified gaps; this would allow editing future versions of this dataset in a few years and potentially help

people better understand the fate of carbon under highly reducing conditions such as the one produced during serpentinization.

ACKNOWLEDGEMENTS

This research is supported by the AP Sloan Foundation through the Deep Carbon Observatory's Deep Energy community and Data Science team (G-2018-11204). S.B. also thanks TOTAL EP R&D Project MAFOOT for financial support. We are grateful to the authors of the 30 publications used for this analysis. We thank Cécile Bourquin and Valentine Megevand for their contribution to completing this dataset. The authors also want to thank the two anonymous reviewers for their fruitful comments that considerably improved the manuscript.





CONFLICT OF INTEREST

The authors declare no conflict of interest.

OPEN PRACTICES

This article has earned an Open Data badge for making publicly available the digitally-shareable data necessary to reproduce the reported results. The data is available at <http://info.deepcarbon.net/individual/n1819> Learn more about the Open Practices badges from the Center for OpenScience: <https://osf.io/tvyxz/wiki>

ORCID

Fang Huang  <https://orcid.org/0000-0002-6017-442X>
 Samuel Barbier  <https://orcid.org/0000-0003-1960-1087>
 Renbiao Tao  <https://orcid.org/0000-0003-4797-5211>
 Jihua Hao  <https://orcid.org/0000-0003-3657-050X>
 Pablo Garcia del Real  <https://orcid.org/0000-0003-2075-0944>
 Steve Peuble  <https://orcid.org/0000-0003-0860-7344>
 Andrew Merdith  <https://orcid.org/0000-0002-7564-8149>
 Jean-Philippe Perrillat  <https://orcid.org/0000-0002-3073-6241>
 Kathy Fontaine  <https://orcid.org/0000-0001-6762-8351>
 Muriel Andreani  <https://orcid.org/0000-0001-8043-0905>

REFERENCES

- Allen, D.E. and Seyfried, W.E. (2003) Compositional controls on vent fluids from ultramafic-hosted hydrothermal systems at mid-ocean ridges: An experimental study at 4 00°C, 500 bars. *Geochimica et Cosmochimica Acta*, 67(8), 1531–1542.
- Andreani, M., Daniel, I. and Pollet-Villard, M. (2013) Aluminum speeds up the hydrothermal alteration of olivine. *American Mineralogist*, 98(10), 1738–1744.
- Barbier, S., Huang, F., Andreani, M., Tao, R., Hao, J., Eleish, A. *et al.* (2020) A review of H₂, CH₄, and hydrocarbon formation in experimental serpentinization using network analysis. *Frontiers in Earth Science*.8, 209. <https://doi.org/10.3389/feart.2020.00209>

- Barnes, I., LaMarche, V.C. and Himmelberg, G. (1967) Geochemical evidence of present-day serpentinization. *Science*, 156(3776), 830–832.
- Berndt, M.E., Allen, D.E. and Seyfried, W.E. (1996) Reduction of CO₂ during serpentinization of olivine at 300°C and 500 bar. *Geology*, 24(4), 351–354.
- Brazil, R. (2017) Hydrothermal vents and the origins of life. *Chemistry World*, 14(5), 48–53.
- Brunet, F. (2019) Hydrothermal production of H₂ and magnetite from steel slags: a geo-inspired approach based on olivine serpentinization. *Frontiers in Earth Science*, 7, 17.
- Charlou, J.L., Donval, J.P., Fouquet, Y., Jean-Baptiste, P. and Holm, N. (2002) Geochemistry of high H₂ and CH₄ vent fluids issuing from ultramafic rocks at the Rainbow hydrothermal field (36°14'N, MAR). *Chemical Geology*, 191(4), 345–359.
- Dufaud, F., Martinez, I. and Shilobreeva, S. (2009) Experimental study of Mg-rich silicates carbonation at 400 and 500°C and 1 kbar. *Chemical Geology*, 265(1–2), 79–87.
- Ehlmann, B.L., Mustard, J.F. and Murchie, S.L. (2010) Geologic setting of serpentine deposits on Mars. *Geophysical Research Letters*, 37(6), 1–5. <https://doi.org/10.1029/2010GL042596>
- Etiopie, G. and Ionescu, A. (2015) Low-temperature catalytic CO₂ hydrogenation with geological quantities of ruthenium: a possible abiotic CH₄ source in chromitite-rich serpentinized rocks. *Geofluids*, 15(3), 438–452.
- Etiopie, G., Ifandi, E., Nazzari, M., Procesi, M., Tsikouras, B., Ventura, G. *et al.* (2018) Widespread abiotic methane in chromitites. *Scientific Reports*, 8(1). <https://doi.org/10.1038/s41598-018-27082-0>
- Evans, B.W., Hattori, K. and Baronnet, A. (2013) Serpentinite: what, why, where? *Elements*, 9(2), 99–106.
- Foustoukos, D.I. and Seyfried, W.E. (2004) Hydrocarbons in hydrothermal vent fluids: The role of chromium-bearing catalysts. *Science*, 304(5673), 1002–1005.
- Fu, Q., Sherwood Lollar, B., Horita, J., Lacrampe-Couloume, G. and Seyfried, W.E. (2007) Abiotic formation of hydrocarbons under hydrothermal conditions: Constraints from chemical and isotope data. *Geochimica et Cosmochimica Acta*, 71(8), 1982–1998.
- Fu, Q., Foustoukos, D.I. and Seyfried, W.E. (2008) Mineral catalyzed organic synthesis in hydrothermal systems: An experimental study using time-of-flight secondary ion mass spectrometry. *Geophysical Research Letters*, 35(7). <https://doi.org/10.1029/2008GL033389>
- Grozeva, N.G., Klein, F., Seewald, J.S. and Sylva, S.P. (2017) Experimental study of carbonate formation in oceanic peridotite. *Geochimica et Cosmochimica Acta*, 199, 264–286.
- Guillot, S. and Hattori, K. (2013) Serpentinites: Essential roles in geodynamics, arc volcanism, sustainable development, and the origin of life. *Elements*, 9(2), 95–98.
- Hellevang, H., Huang, S. and Thorseth, I.H. (2011) The potential for low-temperature abiotic hydrogen generation and a hydrogen-driven deep biosphere. *Astrobiology*, 11(7), 711–724.
- Holm, N.G., Oze, C., Mousis, O., Waite, J.H. and Guilbert-Lepoutre, A. (2015) Serpentinization and the formation of H₂ and CH₄ on celestial bodies (Planets, Moons, Comets). *Astrobiology*, 15(7), 587–600.
- Horita, J. and Berndt, M.E. (1999) Abiogenic methane formation and isotopic fractionation under hydrothermal conditions. *Science*, 285(5430), 1055–1057.
- Huang, R.F., Sun, W.D., Ding, X., Liu, J.Z. and Peng, S.B. (2015) Olivine versus peridotite during serpentinization: Gas formation. *Science China Earth Sciences*, 58(12), 2165–2174.
- Huang, R., Sun, W., Liu, J., Ding, X., Peng, S. and Zhan, W. (2016) The H₂/CH₄ ratio during serpentinization cannot reliably identify biological signatures. *Scientific Reports*, 6(1). <https://doi.org/10.1038/srep33821>
- Huang, R., Sun, W., Song, M. and Ding, X. (2019) Influence of pH on molecular hydrogen (H₂) generation and reaction rates during serpentinization of peridotite and olivine. *Minerals*, 9(11), 661.
- Ji, F., Zhou, H. and Yang, Q. (2008) The abiotic formation of hydrocarbons from dissolved CO₂ under hydrothermal conditions with cobalt-bearing magnetite. *Origins of Life and Evolution of Biospheres*, 38(2), 117–125.
- Jones, L.C., Rosenbauer, R., Goldsmith, J.I. and Oze, C. (2010) Carbonate control of H₂ and CH₄ production in serpentinization systems at elevated P-Ts. *Geophysical Research Letters*, 37(14). <https://doi.org/10.1029/2010GL043769>
- Klein, F. and McCollom, T.M. (2013) From serpentinization to carbonation: New insights from a CO₂ injection experiment. *Earth and Planetary Science Letters*, 379, 137–145.
- Klein, F., Grozeva, N.G., Seewald, J.S., McCollom, T.M., Humphris, S.E., Moskowitz, B. *et al.* (2015) Fluids in the Crust. Experimental constraints on fluid-rock reactions during incipient serpentinization of harzburgite. *American Mineralogist*, 100(4), 991–1002.
- Konn, C., Charlou, J.L., Donval, J.P., Holm, N.G., Dehairs, F. and Bouillon, S. (2009) Hydrocarbons and oxidized organic compounds in hydrothermal fluids from Rainbow and Lost City ultramafic-hosted vents. *Chemical Geology*, 258(3–4), 299–314.
- Kularatne, K., Sissmann, O., Kohler, E., Chardin, M., Noirez, S. and Martinez, I. (2018) Simultaneous ex-situ CO₂ mineral sequestration and hydrogen production from olivine-bearing mine tailings. *Applied Geochemistry*, 95, 195–205.
- Lafay, R., Montes-Hernandez, G., Janots, E., Chiriac, R., Findling, N. and Toche, F. (2012) Mineral replacement rate of olivine by chrysotile and brucite under high alkaline conditions. *Journal of Crystal Growth*, 347(1), 62–72.
- Lazar, C., McCollom, T.M. and Manning, C.E. (2012) Abiogenic methanogenesis during experimental komatiite serpentinization: Implications for the evolution of the early Precambrian atmosphere. *Chemical Geology*, 326–327, 102–112.
- Lazar, C., Cody, G.D. and Davis, J.M. (2015) A kinetic pressure effect on the experimental abiotic reduction of aqueous CO₂ to methane from 1 to 3.5 kbar at 300°C. *Geochimica et Cosmochimica Acta*, 151, 34–48.
- Marcaillou, C., Muñoz, M., Vidal, O., Parra, T. and Harfouche, M. (2011) Mineralogical evidence for H₂ degassing during serpentinization at 300°C/300 bar. *Earth and Planetary Science Letters*, 303(3–4), 281–290.
- Mayhew, L.E., Ellison, E.T., McCollom, T.M., Trainor, T.P. and Templeton, A.S. (2013) Hydrogen generation from low-temperature water-rock reactions. *Nature Geoscience*, 6(6), 478–484.
- McCollom, T.M. (2016) Abiotic methane formation during experimental serpentinization of olivine. *Proceedings of the National Academy of Sciences of the United States of America*, 113(49), 13965–13970.
- McCollom, T.M. and Donaldson, C. (2016) Generation of hydrogen and methane during experimental low-temperature reaction of ultramafic rocks with water. *Astrobiology*, 16(6), 389–406.
- McCollom, T.M. and Seewald, J.S. (2001) A reassessment of the potential for reduction of dissolved CO₂ to hydrocarbons during serpentinization of olivine. *Geochimica et Cosmochimica Acta*, 65(21), 3769–3778.
- McCollom, T.M. and Seewald, J.S. (2003) Experimental study of the hydrothermal reactivity of organic acids and acid anions: II. Acetic

- acid, acetate, and valeric acid. *Geochimica et Cosmochimica Acta*, 67(19), 3645–3664.
- McCullom, T.M. and Seewald, J.S. (2013) Serpentinites, hydrogen, and life. *Elements*, 9(2), 129–134.
- McCullom, T.M., Lollar, B.S., Lacrampe-Couloume, G. and Seewald, J.S. (2010) The influence of carbon source on abiotic organic synthesis and carbon isotope fractionation under hydrothermal conditions. *Geochimica et Cosmochimica Acta*, 74(9), 2717–2740.
- McCullom, T.M., Seewald, J.S. and German, C.R. (2015) Investigation of extractable organic compounds in deep-sea hydrothermal vent fluids along the Mid-Atlantic Ridge. *Geochimica et Cosmochimica Acta*, 156, 122–144.
- McCullom, T.M., Klein, F., Robbins, M., Moskowitz, B., Berquó, T.S., Jöns, N. *et al.* (2016) Temperature trends for reaction rates, hydrogen generation, and partitioning of iron during experimental serpentinization of olivine. *Geochimica et Cosmochimica Acta*, 181, 175–200.
- McCullom, T.M., Klein, F., Solheid, P. and Moskowitz, B. (2020) The effect of pH on rates of reaction and hydrogen generation during serpentinization. *Philosophical Transactions of the Royal Society A*, 378(2165), 20180428.
- McKee, D.W. (1967) Interaction of hydrogen and carbon monoxide on platinum group metals. *Journal of Catalysis*, 8(3), 240–249.
- Melaet, G., Ralston, W.T., Li, C.-S., Alayoglu, S., An, K., Musselwhite, N. *et al.* (2014) Evidence of highly active cobalt oxide catalyst for the Fischer-Tropsch synthesis and CO₂ hydrogenation. *Journal of the American Chemical Society*, 136(6), 2260–2263.
- Ménez, B., Pisapia, C., Andreani, M., Jamme, F., Vanbellingen, Q.P., Brunelle, A. *et al.* (2018) Abiotic synthesis of amino acids in the recesses of the oceanic lithosphere. *Nature*, 564(7734), 59–63.
- Michiels, K., Haesen, A., Meynen, V. and Spooen, J. (2018) Applicability of fine industrial metallic iron-rich waste powders for hydrothermal production of hydrogen gas: The influence of non-ferrous contaminants. *Journal of Cleaner Production*, 195, 674–686.
- Miller, H.M., Mayhew, L.E., Ellison, E.T., Kelemen, P., Kubo, M. and Templeton, A.S. (2017) Low temperature hydrogen production during experimental hydration of partially-serpentinized dunite. *Geochimica et Cosmochimica Acta*, 209, 161–183.
- Neubeck, A., Duc, N.T., Bastviken, D., Crill, P. and Holm, N.G. (2011) Formation of H₂ and CH₄ by weathering of olivine at temperatures between 30 and 70°C. *Geochemical Transactions*, 12(1), 6.
- Neubeck, A., Duc, N.T., Hellevang, H., Oze, C., Bastviken, D., Bacsik, Z. *et al.* (2014) Olivine alteration and H₂ production in carbonate-rich, low temperature aqueous environments. *Planetary and Space Science*, 96, 51–61.
- Okland, I., Huang, S., Thorseth, I.H. and Pedersen, R.B. (2014) Formation of H₂, CH₄ and N-species during low-temperature experimental alteration of ultramafic rocks. *Chemical Geology*, 387(1), 22–34.
- Proskurowski, G., Lilley, M.D., Kelley, D.S. and Olson, E.J. (2006) Low temperature volatile production at the Lost City Hydrothermal Field, evidence from a hydrogen stable isotope geothermometer. *Chemical Geology*, 229(4), 331–343.
- Proskurowski, G., Lilley, M.D., Seewald, J.S., Früh-Green, G.L., Olson, E.J., Lupton, J.E. *et al.* (2008) Abiogenic hydrocarbon production at lost city hydrothermal field. *Science*, 319(5863), 604–607.
- Russell, M.J., Hall, A.J. and Martin, W. (2010) Serpentinization as a source of energy at the origin of life. *Geobiology*, 8(5), 355–371.
- Schulte, M., Blake, D., Hoehler, T. and McCollom, T. (2006) Serpentinization and its implications for life on the early Earth and Mars. *Astrobiology*, 6(2), 364–376.
- Seewald, J.S., Zolotov, M.Y. and McCollom, T. (2006) Experimental investigation of single carbon compounds under hydrothermal conditions. *Geochimica et Cosmochimica Acta*, 70(2), 446–460.
- Seyfried, W.E., Foustoukos, D.I. and Fu, Q. (2007) Redox evolution and mass transfer during serpentinization: An experimental and theoretical study at 200°C, 500 bar with implications for ultramafic-hosted hydrothermal systems at Mid-Ocean Ridges. *Geochimica et Cosmochimica Acta*, 71(15), 3872–3886.
- Sleep, N.H., Meibom, A., Fridriksson, T., Coleman, R.G. and Bird, D.K. (2004) H₂-rich fluids from serpentinization: Geochemical and biotic implications. *Proceedings of the National Academy of Sciences of the United States of America*, 101(35), 12818–12823.
- Stangeland, K., Kalai, D., Li, H. and Yu, Z. (2017) CO₂ methanation: the effect of catalysts and reaction conditions. *Energy Procedia*, 105, 2022–2027.
- Wenner, D.B. and Taylor, H.P. (1973) Oxygen and hydrogen isotope studies of the serpentinization of ultramafic rocks in oceanic environments and continental ophiolite complexes. *American Journal of Science*, 273(3), 207–239.
- Zahnle, K., Freedman, R.S. and Catling, D.C. (2011) Is there methane on Mars? *Icarus*, 212(2), 493–503.

How to cite this article: Huang F, Barbier S, Tao R, et al. Dataset for H₂, CH₄ and organic compounds formation during experimental serpentinization. *Geosci. Data J.* 2021;8:90–100. <https://doi.org/10.1002/gdj3.105>